



12-1969

Transpiration Measurements of the Decomposition Pressures of Barium Hexafluorosilicate

Kemal Cankaya

Follow this and additional works at: https://scholarworks.wmich.edu/masters_theses



Part of the Chemistry Commons

Recommended Citation

Cankaya, Kemal, "Transpiration Measurements of the Decomposition Pressures of Barium Hexafluorosilicate" (1969). *Master's Theses*. 2949.

https://scholarworks.wmich.edu/masters_theses/2949

This Masters Thesis-Open Access is brought to you for free and open access by the Graduate College at ScholarWorks at WMU. It has been accepted for inclusion in Master's Theses by an authorized administrator of ScholarWorks at WMU. For more information, please contact wmu-scholarworks@wmich.edu.



TRANSPIRATION MEASUREMENTS OF THE DECOMPOSITION
PRESSURES OF BARIUM HEXAFLUROSILICATE

by

Kemal Cankaya

A Thesis
Submitted to the
Faculty of the School of Graduate
Studies in partial fulfillment
of the
Degree of Master of Arts

Western Michigan University
Kalamazoo, Michigan
December, 1969

ACKNOWLEDGEMENTS

I wish to thank Dr. Adli S. Kana'an for his friendship, help and instruction through the course of this study. Also, I want to thank the other committee members, Dr. Joseph M. KanamueLLer and Dr. Thomas Houser, for their helpful suggestions. Further, I wish to express my thanks to the faculty and fellow students for their constructive criticism and inspiration. The technical assistance of Mr. Richard Durbin of the machine shop is also acknowledged.

I am indebted to the Turkish Paper and Cellulose Company for the invaluable scholarship which included living and schooling expenses. This scholarship gave me the opportunity for undergraduate and graduate studies in the United States of America.

Lastly, I would like to thank the Chemistry Department at Western Michigan University for their additional support by granting me a teaching assistantship during my graduate studies.

Kemal Cankaya

MASTER'S THESIS

M-2283

CANKAYA, Kemal

TRANSPIRATION MEASUREMENTS OF THE DECOMPOSITION
PRESSURES OF BARIUM HEXAFLUROSILICATE.

Western Michigan University, M.A., 1970
Chemistry, physical

University Microfilms, A XEROX Company, Ann Arbor, Michigan

TABLE OF CONTENTS

CHAPTER		PAGE
	INTRODUCTION	1
I	THEORY	3
	The Transpiration Method	3
	Principles and Limitations of the Method . . .	4
	Diffusion and Kinetic Effects	5
	Identification of Vapor Species	7
II	EXPERIMENTAL	9
	Description of Apparatus	9
	Gas Purification System	9
	Flow Manifold	9
	Transpiration Assembly	11
	The Furnace and Temperature Control and Measurement.	13
	Calibration of the Experimental Thermocouple .	15
	Procedures	17
III	DECOMPOSITION PRESSURES AND THERMODYNAMIC PRO- PERTIES OF BARIUM HEXAFLUOROSILICATE, BaSiF_6 . .	19
	Material	19
	Measured Quantities	19
	Results	21
	Error Analysis	29
	Derived Thermodynamic Properties	30

TABLE OF CONTENTS (Continued)

	PAGE
Discussions and Conclusions	32
Recommendations for Future Work	34
APPENDICES	36
Appendix A: Flowmeter Calibration	37
Appendix B: Temperature Profile in the Reaction Region of the Furnace .	39
Appendix C: Calibration of the Experimental- and Reference- Thermocouples . .	40
Appendix D: Analysis of Barium Hexafluoro- silicate	42
BIBLIOGRAPHY	46

LIST OF TABLES

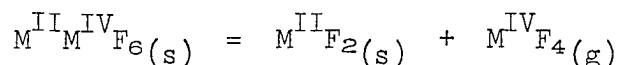
TABLE		PAGE
I	Effect of Flow Rate of Argon on the Weight Loss of BaSiF_6 at 650°K	22
II	Effect of Flow Rate of Argon on the Weight Loss of BaSiF_6 at 690°K	22
III	Transpiration Data for the Reaction: $\text{BaSiF}_6(\text{s}) = \text{BaF}_2(\text{s}) + \text{SiF}_4(\text{g})$	26
IV	Decomposition Pressures of SiF_4 over BaSiF_6 . . .	27
V	Flowmeter Calibration at Experimental Conditions.	38
VI	Calibration of the Experimental Thermocouple in the Transpiration Furnace Against the Reference Thermocouple	41
VII	Calibration of the Reference Thermocouple Against the Standard Thermocouple	41
VIII	X-Ray Diffraction Data of BaSiF_6 Sample Prior to Decomposition	44
IX	X-Ray Diffraction Data of BaSiF_6 Sample after Decomposition	45

LIST OF FIGURES

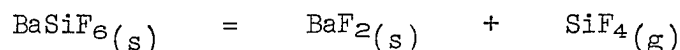
FIGURE		PAGE
1	Variation of the Mole Fraction of Transported Vapor with the Flow Rate	6
2	Flow Manifold	10
3	Transpiration Assembly	12
4	High Temperature Furnace for Transpiration Studies	14
5	Effect of Flow Rate of Argon on the Weight Loss of BaSiF ₆ at 650°K	23
6	Effect of Flow Rate of Argon on the Weight Loss of BaSiF ₆ at 690°K	24
7	Temperature Dependence of the Equilibrium Constant of BaSiF ₆ Decomposition	28

INTRODUCTION

The relatively stable, complex fluorides at room temperature of formula $M^{II}M^{IV}F_6$ (where M^{II} : Mg, Ca, Sr, Ba; M^{IV} : Si, Ge, Sn, Ti, Zr) offer interesting possibilities as a source of $M^{IV}F_4$. At high temperatures such compounds decompose according to the reaction:



However, the thermodynamic properties of such reactions have been established only in a few cases. Of particular interest is barium hexafluorosilicate, $BaSiF_6$, which is known to decompose according to the above equation¹ and is used as a source of high purity silicon tetrafluoride.² The thermal stability of $BaSiF_6$ had been investigated by Deadmore et.al.³ in dry air using differential thermal analysis and isothermal weight loss measurements. The activation energy of the decomposition reaction:

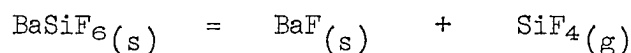


calculated from the weight loss versus time data was 32.8 kcal mole⁻¹. The reported information did not establish the thermodynamic properties of $BaSiF_6$ or its decomposition reaction.

The purpose of this research was to study equilibrium decomposition pressures of silicon tetrafluoride over barium hexafluorosilicate and to establish some of the thermodynamic properties of the latter compound. In this study the transpiration method was used to determine the decomposition pressures in the temperature range

618-691°K. This method was selected in preference to the Knudsen effusion since it was expected that the decomposition pressures would not be within the pressure range (10^{-2} - 10^{-6} Torr) of the applicability of the Knudsen equation. The static method, on the other hand, is more convenient for decomposition reactions which are known to be relatively slow in establishing equilibrium, which is not the case in the present study.

The equilibrium constant for the decomposition of BaSiF_6 :



is given by the equation

$$K_p = p_{\text{SiF}_4}$$

The enthalpy and entropy of decomposition, ΔH_T° and ΔS_T° respectively were calculated from the van't Hoff relation⁴ and the definition of ΔG° were utilized in evaluating some of the thermodynamic properties of barium hexafluorosilicate.

CHAPTER I

THEORY

The Transpiration Method

The transpiration method is an established and useful method for the study of gas-solid or gas-liquid equilibria. Regnault,⁵ a French chemist and physicist, is credited by Thomson⁶ as the originator of this method in 1845. Its primary use is to measure vapor and dissociation pressures, for which it is well suited since data can be obtained in the presence of large concentrations of foreign gases, and over a wide range of vapor pressures (0.01 to 50 Torr). A recent review by Merten and Bell⁷ outlines the general principles, applications and limitations of the transpiration method.

In the transpiration method of vapor or dissociation pressure measurements, a steady stream of a gas, which may be either inert or reactive, is passed over a condensed sample, which is held under isothermal conditions. The flow rate of the carrier gas should be sufficiently low to ensure equilibrium with the sample, but it should be fast enough so that vapor diffusion does not contribute significantly to the vapor transport. The rate of removal of the vapor, above the condensed sample, by the carrier gas, depends on the partial pressure and on the flow rate of the latter, as discussed later.

The vapor or dissociation partial pressures of the vaporizing or dissociating components of the sample are determined from the amount of the transported vapor. This is normally accomplished by

analysis of the collected vapor downstream from the sample or by measurement of the weight loss of the sample. The relationships used to calculate the partial pressures, assuming ideal gas behavior are:

$$P = \sum_i p_i \quad (\text{I-1})$$

$$n = \sum_i n_i \quad (\text{I-2})$$

$$p_v = \frac{n_v}{n_v + n_c} P \quad (\text{I-3})$$

where p_i and n_i are the partial pressure and number of moles of the i th gaseous species respectively, P and n are the total pressure and the total number of moles of gases in the system and the subscripts v and c represent the vapor and carrier gas respectively.

Principles and Limitations of the Method

Transpiration experiments are successful, in terms of the accuracy and reproducibility of their results, only when the following criteria are met: 1) the flow rates of the carrier gas should be of the optimum value required to establish equilibrium in the reaction zone; 2) the temperature of all reagents participating in the reaction must be the same; 3) the measured total pressure must be the pressure in the system; 4) equilibrium in the reaction zone must be maintained throughout the period of the experiment; and 5) the activity of the condensed phase and the sample surface must not change appreciably during a given run.

Most of these criteria can be met by a careful design of the transpiration system and the furnace and by proper selection of the flow rate of the carrier gas and of a sufficiently large sample surface

area. However the usefulness of the method is still hampered by certain experimental limitations, some of which can be controlled. Stable temperatures during an experiment and elimination of temperature gradients over short distances in a supposedly isothermal region are not easily attained. Even in the most carefully designed systems temperature uncertainties range from $\pm 1^\circ$ at 500°C to $\pm 4^\circ$ at 1500°C . At high temperatures, gradients of several degrees may exist. Side reactions with the system and the sample container are often hard to prevent, and identity of the molecular formula of the vapor species must be known. Methods for determining molecular formulas will be discussed in a later section.

Diffusion and Kinetic Effects

Diffusion and kinetics aspects of the transpiration method were discussed by Merten and Bell⁷. The diffusion effects were categorized as ordinary and thermal, and the kinetic effects as saturation effects. The difficulties of correcting for such effects may be eliminated by representing the weight loss as a function of flow rates by curves like that shown in Figure 1. Experiments performed with flow rates corresponding to the plateau region need no correction for diffusion or kinetic effects. In this region the mole fraction of the vapor species, $\frac{n_v}{n_v + n_c}$, as well as the partial pressure calculated from equation (I-3) are independent of the flow rate. At low flow rates vapor diffusion contributes significantly to the number of moles of transported vapor, n_v , and eventually leads to an apparent high partial pressure. At high flow rates n_v and $\frac{n_v}{n_v + n_c}$ become

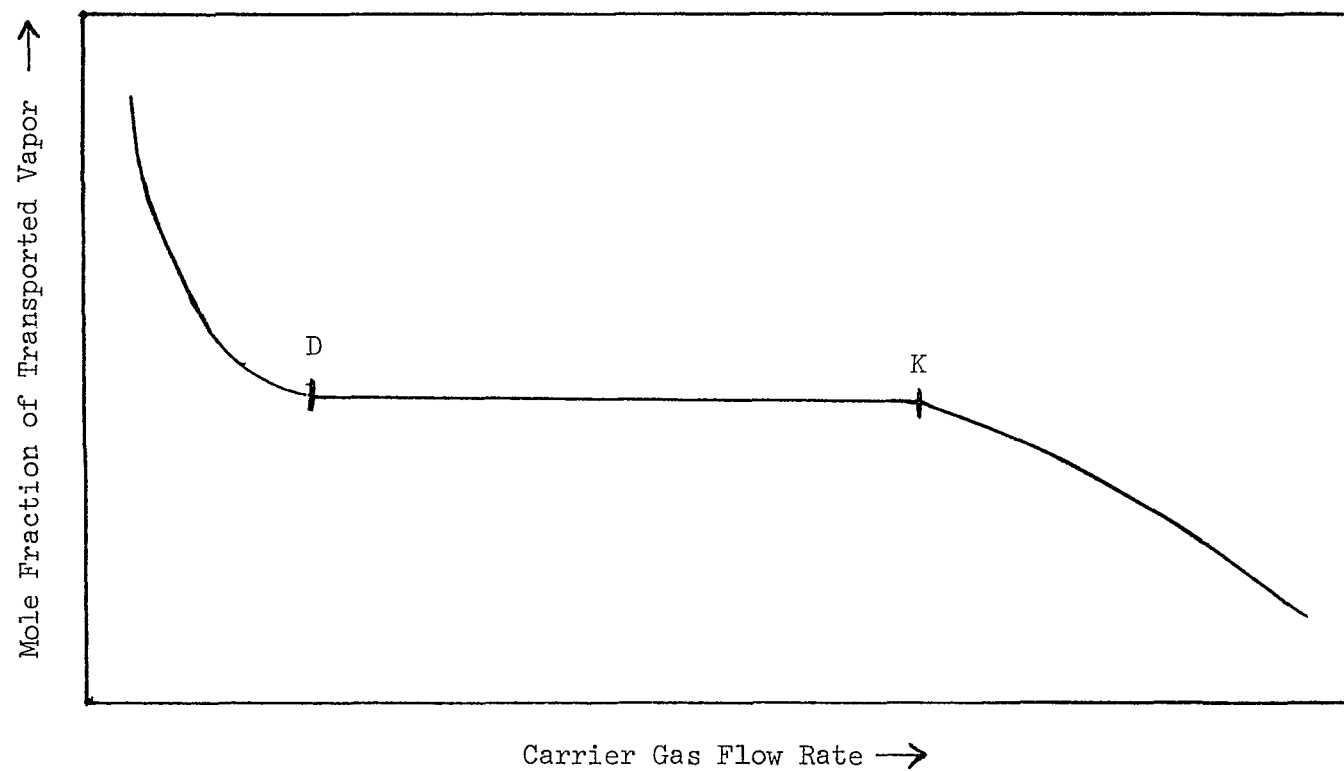


FIGURE 1

Variation of the Mole Fraction of Transported Vapor
with the Flow Rate

small because kinetic limitations prevent saturation of the carrier gas.

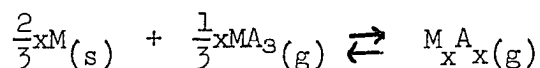
The flow rate range of the plateau region varies according to the experimental arrangement and the system under investigation. Failure to find a plateau region and a continuous increase of the partial pressure at decreasing flow rates is an indication of improper design. The extrapolation of such data to zero flow rate leads to erroneous pressure.

In summary, diffusion effects set a lower limit and kinetic effects set an upper limit on the flow rates that may be used in the transpiration method. These limits are designated by the end points of the plateau, D and K, in Figure 1.

Identification of Vapor Species

The identity of the vapor species is essential to interpret data from pressure measurements by the transpiration method. In many cases, auxiliary techniques such as vapor density, mass spectrometry and optical measurements can be used for this purpose. In certain cases the transpiration method itself serves to establish the identity of vapor species.

One way by which the transpiration method can aid in establishing the identity of vapor species in an equilibrium reaction is by variation of the pressure of a reactive gas. For example in the reaction:



the vapor species can be identified from the slope of the logarithm of the partial pressure of M_xA_x vs. that of the partial pressure of MA_3 .

The expression for the equilibrium constant of the above reaction yields:

$$\log p_{M_x A_x} = \frac{1}{3} x \log p_{MA_3} + \log K \quad (I-4)$$

where x may be evaluated from the slope, $\frac{x}{3}$. In the case of complex reactions where more stoichiometric variables are involved, the reactions may be represented by several different equilibrium constants and these can be solved simultaneously. Specific examples are cited in the literature⁸⁻¹².

CHAPTER II

EXPERIMENTAL

Description of Apparatus

The experimental apparatus used in transpiration studies of decomposition pressures consisted of a gas purification system, a flow manifold, a transpiration assembly and a furnace and temperature control and measurement assembly.

Gas Purification System

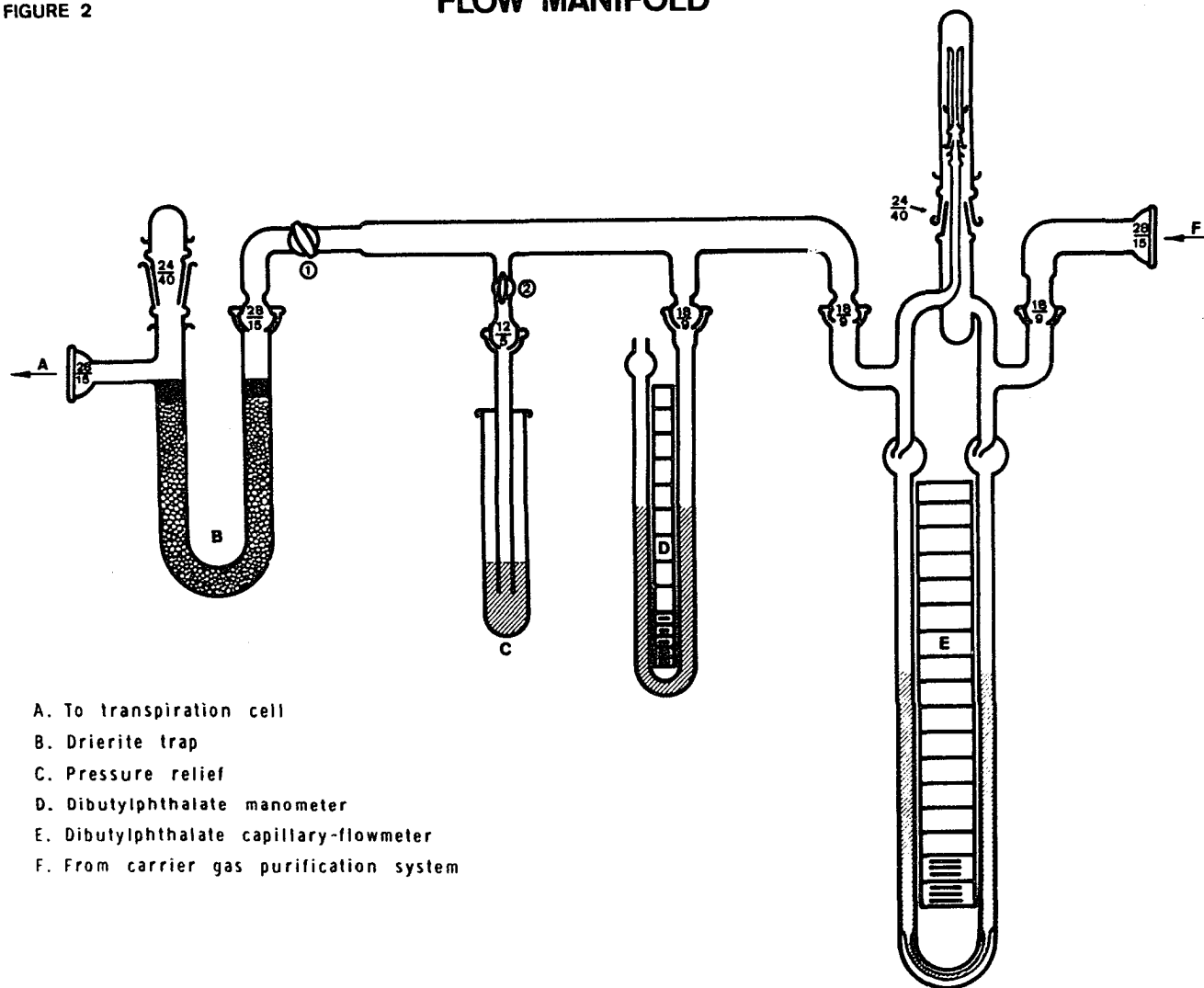
The carrier gas, argon, was dried over Drierite in a drying tower and deoxygenated by passing over copper turnings in a quartz tube heated at 650°C by a tubular furnace (Hoskins Type FD303).

Flow Manifold

A schematic of the flow manifold is shown in Figure 2. The flow of purified carrier gas was regulated by a needle valve, downstream of the purification system. Before entering the transpiration system, the flow rate was measured by a calibrated capillary flowmeter, E (Appendix A). The pressure difference from barometric pressure, in the system, was measured by a dibutylphthalate manometer, D. A pressure relief arrangement, C, a drying tower of Drierite, B, and a connecting tube fitted with a ball joint, A, conduct the carrier gas to the transpiration assembly. A thermometer placed inside a glass tube, which

FIGURE 2

FLOW MANIFOLD



- A. To transpiration cell
- B. Drierite trap
- C. Pressure relief
- D. Dibutylphthalate manometer
- E. Dibutylphthalate capillary-flowmeter
- F. From carrier gas purification system

connects the purification system to the flow manifold, measures the temperature of the carrier gas.

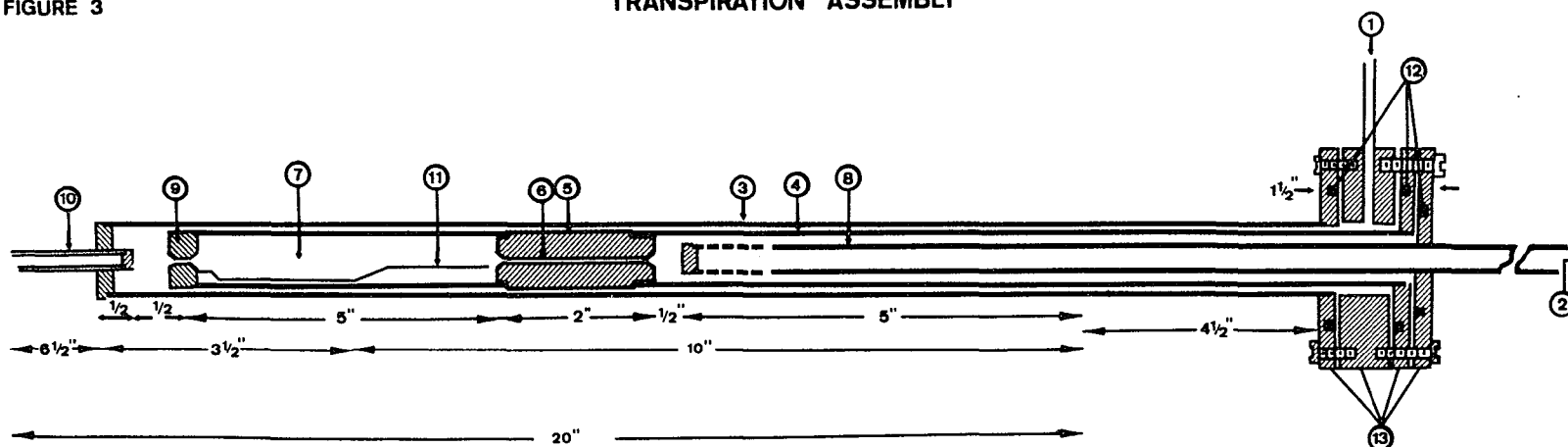
Transpiration Assembly

The transpiration assembly, shown in Figure 3, was constructed of Monel and nickel. It consisted of a housing tube, 3, enclosing an inner composite tube. The housing tube was fitted at one end with a closed monel tube 1/8 inch in diameter, used as a well for the experimental thermocouple, 10. The other end of the housing tube was silver soldered to an o-ring brass-flange, 13.

The composite tube consisted of two sections: a reaction cell, 7, and a condenser, 8. The two sections were joined by taper joints machined into one end of the cell and a nickel rod, 5, welded to one end of the condenser. The vapor from the reaction cell was admitted to the condenser jacket, 4, through a capillary (1 mm in diameter and 5 cm long), 6, drilled in the tapered nickel rod. The carrier gas entered the reaction cell through a hole (1 mm in diameter) in a detachable tapered cap, 9, at the inlet of the reaction cell. Inlet of the carrier gas to the assembly was through a brass tube, 1, fitted to a brass ring located between brass flanges on both tubes. All permanent connections of the assembly components in the hot region were Heli-arc welded. The assembly was leak free due to the o-ring flanges shown in Figure 3.

FIGURE 3

TRANSPIRATION ASSEMBLY



- | | |
|-------------------------------------|--------------------------------|
| 1. Argon input | 8. Monel condenser |
| 2. Argon output | 9. Nickel entrance-cap |
| 3. Monel housing-tube | 10. Thermo couple well (Monel) |
| 4. Condenser jacket-tube (Monel) | 11. Nickel sample-boat |
| 5. Nickel insert for capillary tube | 12. Neoprene o-rings |
| 6. Stainless steel capillary-tube | 13. Brass flanges |
| 7. Monel reaction-cell | |

The Furnace and Temperature Control and Measurement

The furnace and temperature control

The transpiration assembly was heated by a wire-wound resistance furnace shown in Figure 4. The core was a Mullite tube 2.75 inches i.d., 3 inches o.d., and 20 inches long. The heating element was B and S 15 gauge Kanthal A-1 wire, wound over the middle 16 inches of the Mullite tube. The windings were closely separated towards the ends to compensate for heat losses and to help maintain a relatively long isothermal hot zone. A stainless steel core, a second mullite tube and the transpiration assembly were inserted in the furnace tube in the mentioned order. The stainless steel core (2.375 inches o.d., 1.5 inches i.d., and 12 inches long) served as a heat sink to reduce temperature gradient in the reaction cell. The furnace tube was housed in a cold-rolled steel shell 8 inches in diameter and 20 inches long. Size 20 abrasive grain Norton Alundum was used for insulation. The furnace was capped at both ends with Transite plates.

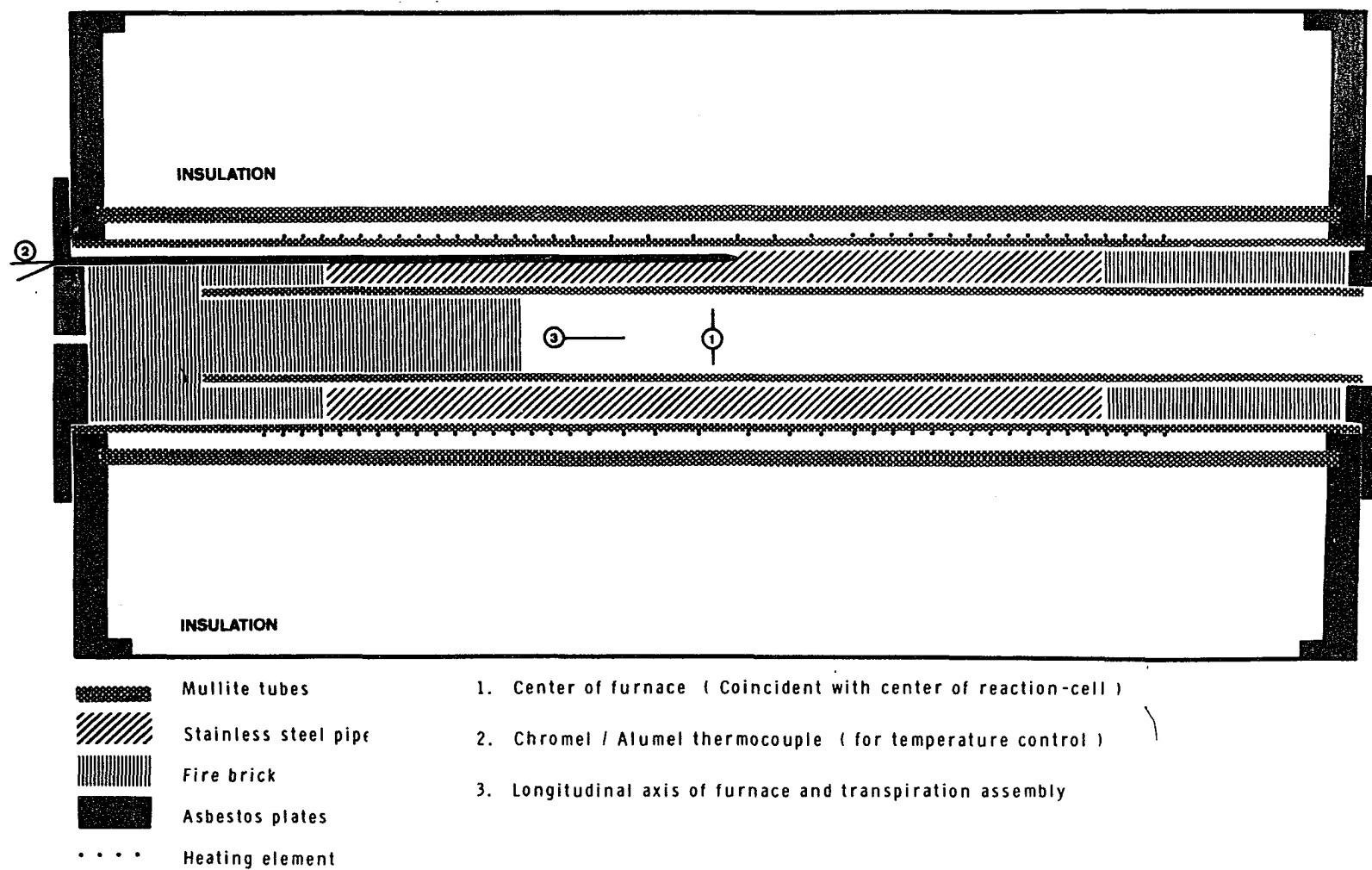
The furnace temperature was controlled by a time-proportioning controller (Honeywell Versatronic, Model R 7161H) actuated by a Chromel-Alumel thermocouple, 2, embedded in a 1/8 inch groove in the stainless steel core.

Temperature measurement

A Chromel-Alumel thermocouple inserted along the furnace axis in the thermocouple well, with its junction near the reaction cell entrance, was used to measure the sample temperature. The thermocouple output was

FIGURE 4

HIGH TEMPERATURE FURNACE FOR TRANSPIRATION STUDIES



measured by a portable precision potentiometer (Honeywell Model 2745). The relation between the output of the experimental thermocouple and the sample temperature in the reaction cell was established by calibration against a precalibrated thermocouple, as described in the next section.

At thermal equilibrium the temperature profile discussed in Appendix B, indicates that the temperature of the sample in the reaction cell was known to $\pm 2.5^\circ$. Gas flow rates up to 20 cc/min. had no observable effect on the temperature pattern. This indicates that argon was heated sufficiently during its entrance to the reaction cell.

Calibration of the Experimental Thermocouple

The relation between the output of the experimental thermocouple, used for temperature measurements in an experiment, and the sample temperature in the reaction cell was established by calibration against a precalibrated thermocouple. The precalibrated thermocouple referred to as the "reference thermocouple", was placed inside the reaction cell in a position corresponding to that of the center of the sample. The cold junctions of the two thermocouples, were at the reference temperature of 0°C in the same ice-water bath. The emf outputs of both thermocouples were read by the same potentiometer under the same conditions of a normal experiment. The comparison of the two thermocouples was over the range of temperatures used in the transpiration studies (340 to 420°C). The relation between the emf outputs of the two thermocouples was fitted into a linear equation by least-squares

analysis according to:

$$V_x = A_1 + B_1 V_r \quad (\text{II-1})$$

where V_x and V_r are in millivolts and A_1 and B_1 are -0.447 ± 0.036 and 1.037 ± 0.0023 respectively. The calibration data are presented in (Appendix C).

The reference thermocouple was calibrated against a standard thermocouple (Appendix C). The relation between the emf outputs of the reference and standard thermocouples, from the linear least-squares analysis of the data is:

$$V_r = A_2 + B_2 V_s \quad (\text{II-2})$$

where A_2 and B_2 are 0.403 ± 0.021 and 0.985 ± 0.0014 respectively.

The standard thermocouple was standardized against the freezing temperatures of lead, zinc, aluminum and copper. The resulting standardization of temperature vs. emf of the standard thermocouple is given by the linear equation.

$$T(^{\circ}\text{K}) = A_3 + B_3 V_s \quad (\text{II-3})$$

where A_3 and B_3 are 289.170 ± 0.562 and 23.490 ± 0.028 respectively.

The final equation for the sample temperature in the reaction cell in terms of the emf of the experimental thermocouple was derived by the proper substitutions for V_s in equation (II-3) from equations (II-2) and (II-1) to give:

$$T(^{\circ}\text{K}) = A + B V_x \quad (\text{II-4})$$

where $A = 289.835 \pm 1.15$ and $B = 22.997 \pm 0.066$ respectively. The propagated error in A and B and the estimated precision of measurements of V_x yield an estimated error of $\pm 1.6^{\circ}$ in the temperature. The mean fluctuation of all temperatures measured was $\pm 0.6^{\circ}$.

Procedures

Prior to an experiment the following preparations were made.

1. The housing tube was placed inside the furnace. The gas inlet was connected to the flow manifold. A rapid stream of argon passed through the tube to displace the air.

2. The furnace was heated to a desired temperature.

3. While the furnace was heated a dry sample of BaSiF_6 was placed into a preweighed nickel boat inside an argon-filled polyethylene glove-bag. The loaded boat was reweighed. Prior to use the boat was heated at 250°C and cooled in a dessicator.

4. The loaded boat was inserted in the reaction cell of the composite tube. The latter was capped.

5. The gas flow through the housing tube was discontinued by closing stopcock 1 (in Figure 2) and opening stopcock 2.

6. The composite tube was inserted in position, in the housing tube, while the latter was still in the furnace. The components of the transpiration assembly were fastened by tightening its flanges. The sample was allowed to establish thermal equilibrium in the furnace hot zone for thirty minutes, without flow of argon.

7. Argon flow was adjusted to the desired rate for an experiment by a needle valve.

A partial pressure determination was started as follows.

- a) Argon flow was directed into the transpiration assembly by closing stopcock 2 and opening stopcock 1 simultaneously. At this point an electric timer was started.

b) The flowmeter, manometer, the carrier gas thermometer, the potentiometer and the barometric pressure were all noted and recorded.

c) Argon flow was continued for the desired duration of an experiment. The above readings were noted every fifteen minutes and recorded.

d) At the end of an experiment the transpiration assembly was pulled out of the furnace and allowed to cool under argon atmosphere at a lower flow rate.

e) After cooling to room temperature the transpiration assembly was opened, the sample boat was transferred to a dessicator.

f) The sample boat was weighed for weight loss determination. The boat was emptied, cleaned and reweighed for a check on changes in its weight. The changes were insignificant (less than 0.1 mg).

CHAPTER III

DECOMPOSITION PRESSURES AND THERMODYNAMIC PROPERTIES OF BARIUM HEXAFLUROSILICATE, BaSiF_6

Material

Barium hexafluorosilicate used in this work was a sample of the commercially available compound from Alpha Inorganics, Inc. X-ray powder patterns and atomic emission spectra of the sample (Appendix D), showed the presence of calcium as an impurity. However the sensitivity of the x-ray method is questionable for detection of impurities of the order of 10% or less. Quantitative analysis of the dried sample for barium, silicon, fluorine and calcium by Midwest Microlab, Inc., accounted for 91.3% with the deficiency attributed to oxygen, probably as oxides of silicon, barium and calcium as discussed later. Samples used in the transpiration study were dried to constant weight under vacuum for 24 hours or in air for 70 to 90 hours at 220°C. The weight loss in both treatments amounted to 1.2%.

Measured Quantities

In a typical transpiration experiment for determination of the decomposition pressure of BaSiF_6 the following variables were measured: temperature of argon (carrier gas), flow rate of argon, the total pressure in the system, temperature of BaSiF_6 , time of flow and the weight loss of BaSiF_6 .

Temperature variations of the carrier gas at the flowmeter inlet during an experiment were of the order of $\pm 0.5^\circ$. The total pressure in the system was calculated from the barometric pressure, measured on a standard laboratory barometer, and the pressure difference from barometric pressure, measured by the oil manometer in the flow manifold.

The total weight of SiF_4 transported, was determined from the net weight loss of the sample during the period of argon flow in a given experiment. For a period of 30 minutes, after inserting the sample in the furnace, and prior to starting the flow of argon, the sample loses weight. Also after removing the sample from the furnace, the sample loses weight, while cooling to room temperature. This weight loss, prior to the beginning of argon flow and while cooling is subtracted from the total weight loss to obtain the net weight loss used in the calculations. For each temperature at which decomposition studies were made, this correction was determined in a separate preliminary experiment. In such preliminary experiments the general procedure was followed without the flow of argon during the heating period of 30 minutes, required for the sample to establish thermal equilibrium. At the end of this period the transpiration assembly was pulled out from the furnace and argon flow at relatively low rate was started, while the sample was cooled to room temperature. The weight loss in such a preliminary experiment represents the correction for the weight loss at the respective temperature.

Results

Effect of flow rate on weight loss

To secure a proper flow rate for equilibrium conditions, several experiments at different flow rates were performed to establish the plateau region in the plot of the weight loss of sample per cc of Argon vs. the flow rate of Argon. The data at 690° and 650°K are presented in Tables I and II and Figures 5 and 6.

Decomposition pressure data

The decomposition pressure of $\text{SiF}_4(\text{g})$ over BaSiF_6 was calculated, assuming that the ideal gas law holds in the equilibrium zone, according to:

$$p_{\text{SiF}_4} = \frac{n_{\text{SiF}_4}}{n_{\text{SiF}_4} + n_{\text{Ar}}} P_x \quad (\text{III-1})$$

where the terms are the same as those of equation (I-3). The number of moles of SiF_4 , n_{SiF_4} and of Argon, n_{Ar} were calculated according to:

$$n_{\text{SiF}_4} = \frac{\Delta W}{M} \quad (\text{III-2})$$

and

$$n_{\text{Ar}} = \frac{Q P}{T_{\text{Ar}}} \cdot \frac{273 \cdot 15 t}{(760)(22.414)} \quad (\text{III-3})$$

where ΔW is the weight loss in g; M the molecular weight of SiF_4 ; Q the flow rate in cc min^{-1} under experimental conditions; t duration of flow in minutes; P the total pressure of the system in Torr; T_{Ar} argon temperature in °K.

TABLE I

Effect of Flow Rate of Argon on the Weight Loss
of BaSiF₆ at 650°K

Flow Rate of Ar (cc/min) STP	Total Volume of Ar(cc)	Wt. Loss of BaSiF ₆ Total (mg)	(mg/cc) × 10 ² STP	Ar Temp. at Flowmeter (°K)	Total Pressure in the System (Torr)
8.75	1575	14.3	0.908	306.0	742.5
10.58	1895	18.1	0.955	306.2	743.4
12.04	2172	20.4	0.939	308.2	741.3
7.47	1350	17.7	1.311	305.1	742.5
13.90	2503	19.3	0.771	299.5	742.8

TABLE II

Effect of Flow Rate of Argon on the Weight Loss
of BaSiF₆ at 690°K

Flow Rate of Ar (cc/min) STP	Total Volume of Ar(cc)	Wt. Loss of BaSiF ₆ Total (mg)	(mg/cc) × 10 ² STP	Ar Temp. at Flowmeter (°K)	Total Pressure in the System (Torr)
10.70	642	37.4	5.825	302.5	741.7
12.67	785	44.0	5.605	304.5	741.9
13.45	844	47.4	5.619	303.5	739.9
14.10	835	42.6	5.099	303.6	739.7
14.57	950	53.5	5.634	305.3	738.6
8.53	514	38.3	7.456	303.6	736.0

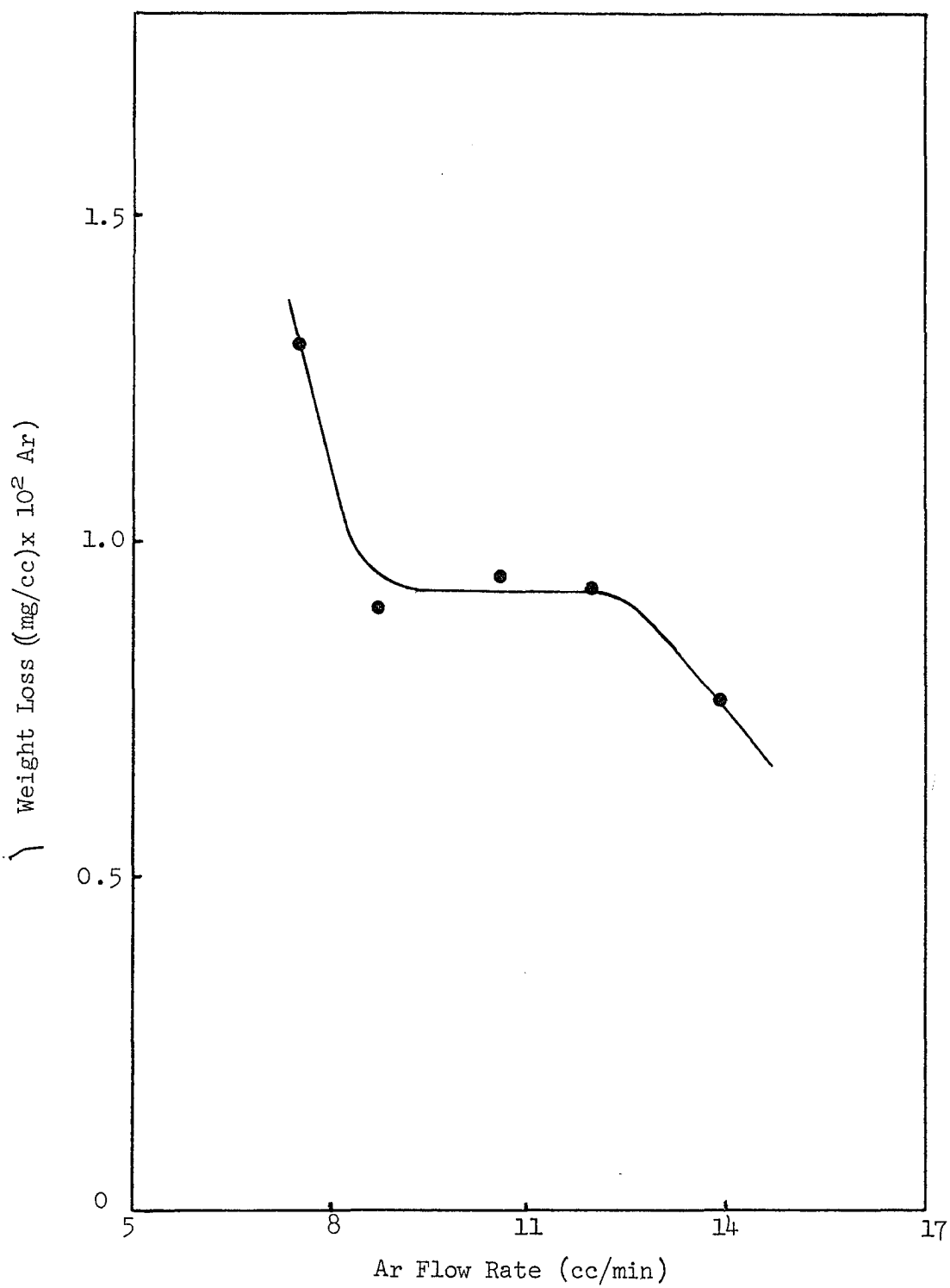


FIGURE 5
Effect of Flow Rate of Argon on the Weight Loss of
 BaSiF_6 at 650°K

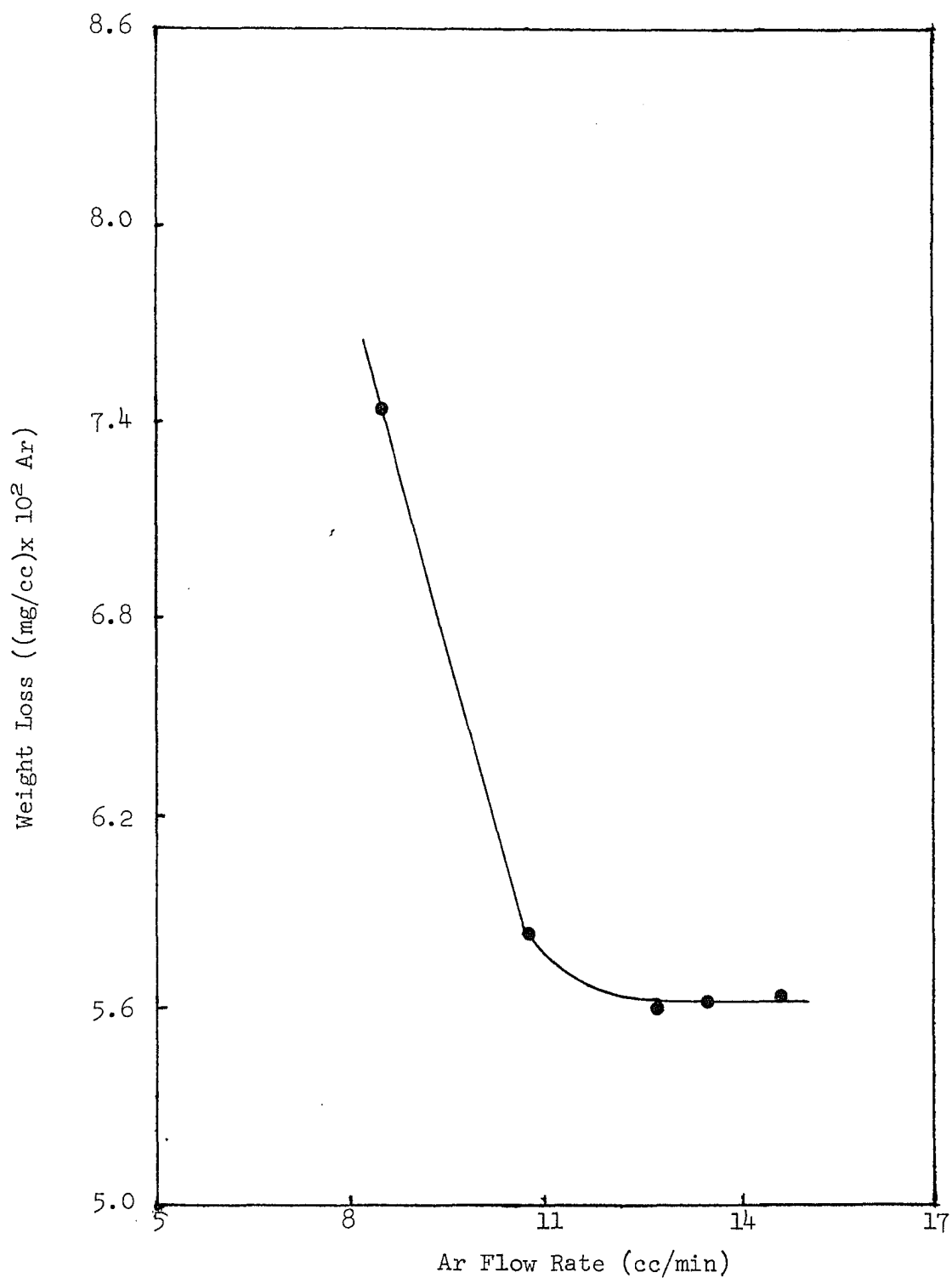


FIGURE 6

Effect of Flow Rate of Argon on the Weight Loss of
 BaSiF_6 at 690°K

The transpiration data and the calculated decomposition pressures for the temperature range 618 to 691°K and for the flow rates, where equilibrium is assumed to be established, are presented in Tables III and IV.

Assuming an activity of unity for $\text{BaSiF}_6(\text{s})$ and $\text{BaF}_2(\text{s})$, the equilibrium constant at a given temperature is represented by the partial pressure of SiF_4 at the respective temperature:

$$K_p(T) = P_{\text{SiF}_4} \quad (\text{III-4})$$

The temperature dependence of the equilibrium constant is shown in Figure 7. A least squares analysis of $\log K$ vs. T^{-1} computed by an IBM 1620 Computer gave:

$$\log K_p = (-8238 \pm 183)T^{-1} + (9.978 \pm 0.120) \quad (\text{III-5})$$

The standard deviation in $\log K_p$ is ± 0.022 . The calculated enthalpy and entropy of the decomposition reaction at the median temperature (655°K) are $\Delta H^\circ = 37.67 \pm 0.84 \text{ kcal mole}^{-1}$ and $\Delta S^\circ = 45.65 \pm 0.55 \text{ eu}$. The reported errors are standard deviations obtained from the least squares analysis.

The effect of BaF_2

The effect of BaF_2 formed during an experiment was tested by mixing BaSiF_6 with BaF_2 . In one experiment at 649°K with 13.66 mole % BaF_2 added, a decrease in the decomposition rate of 16% was observed. However, this effect at the various stages of an experiment starting with BaSiF_6 is not significant, as indicated from the reproductibility of the data.

TABLE III

Transpiration Data for the Reaction: $\text{BaSiF}_6(\text{s}) = \text{BaF}_2(\text{s}) + \text{SiF}_4(\text{g})$

Sample Temp. (°K)	Flow Rate of Ar (cc/min)	Duration of expt. (min)	Weight Loss of BaSiF_6 (mg)	Wt. Loss per cc of Argon (mg/cc) $\times 10^2$	Total Pressure P (Torr)
621.5	10.46	360.05	10.1	0.266	744.2
622.6	10.14	339.04	8.8	0.256	741.5
640.3	9.16	241.83	12.9	0.593	740.9
640.1	8.23	240.02	12.1	0.612	737.5
650.6	12.04	180.05	20.4	0.939	741.3
648.1	10.58	179.13	18.1	0.955	743.4
648.8	8.75	180.00	14.3	0.908	742.5
679.6	11.62	119.33	46.3	3.338	736.6
677.6	10.70	124.00	39.1	2.948	735.9
691.4	14.57	65.12	53.5	5.634	738.6
691.4	13.45	62.74	47.4	5.619	739.9
689.5	12.67	61.92	44.0	5.605	741.9

TABLE IV

Decomposition Pressures of SiF_4 over BaSiF_6

Temperature (°K)	$T^{-1} \times 10^3$ (°K ⁻¹)	Volume of Ar at STP (cc)	Moles of Ar ($\times 10^2$)	Moles of SiF_4 ($\times 10^4$)	Partial Pressure of SiF_4 (atm $\times 10^3$)	$-\log P_{\text{SiF}_4}$
621.5	1.609	3789	16.903	0.970	0.5618	3.250
622.6	1.606	3438	15.340	0.845	0.5374	3.270
640.3	1.562	2177	9.711	1.239	1.2425	2.906
640.1	1.562	1975	8.812	1.162	1.2784	2.893
650.6	1.537	2172	9.692	1.960	1.9684	2.706
648.1	1.543	1895	8.454	1.739	2.0078	2.697
648.8	1.541	1575	7.028	1.374	1.9061	2.720
679.6	1.471	1387	6.188	4.448	6.9167	2.160
677.6	1.476	1326	5.917	3.756	6.1084	2.214
691.4	1.446	950	4.236	5.140	11.6492	1.934
691.4	1.446	844	3.764	4.554	11.6381	1.934
689.5	1.450	785	3.502	4.227	11.6425	1.934

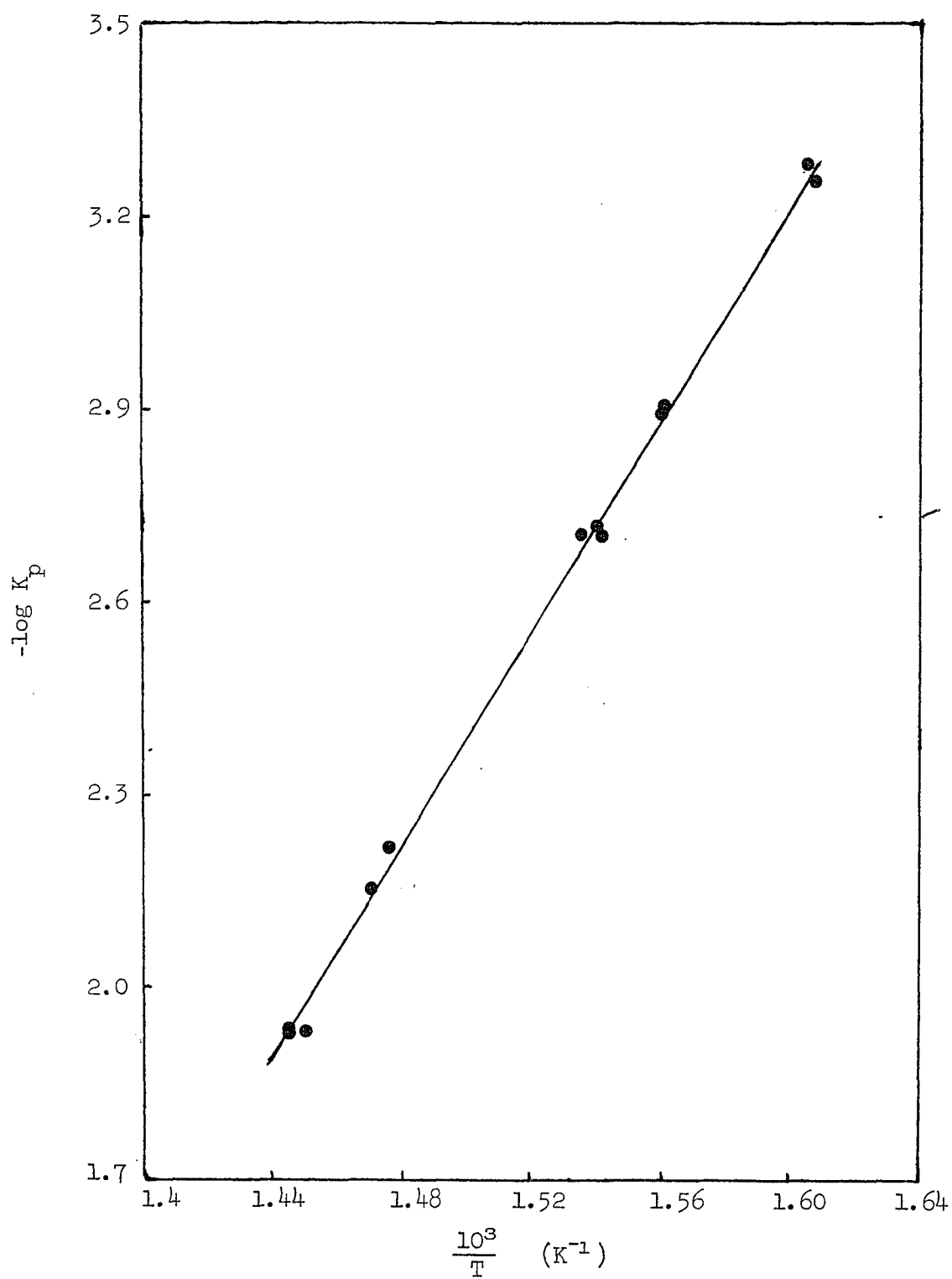


FIGURE 7

Temperature Dependence of the Equilibrium Constant of
 BaSiF_6 Decomposition

Error Analysis

The errors in the measured partial pressure of SiF_4 in equilibrium with barium hexafluorosilicate and its temperature dependence are of two types. The first type is introduced by uncertainties in the measured variables: the flow rate of carrier gas, the weight loss of the sample, the total pressure in the system, the duration of the experiment and the temperatures of the carrier gas and the sample. The second type of error lies in the transpiration method itself where equilibrium is assumed to be established and the assumption of ideal behavior of SiF_4 under the conditions of the experiment.

The propagated error in the partial pressure is mainly due to uncertainties in the flow rate of argon ($\pm 1.6\%$ at high flow rates and $\pm 2.8\%$ at low flow rates) and in the weight loss of the sample ($\pm 1\%$). This propagated error amounts to a mean percent error of $\pm 3.5\%$ in comparison with $\pm 4.1\%$ from the least squares analysis of the data.

The propagated error in the sample temperature is mainly due to temperature fluctuations during a given experiment and to the precision of the potentiometer. A deviation of less than $\pm 0.7^\circ$ was observed in all experiments except one experiment where a deviation of $\pm 2^\circ$ was observed. The uncertainty in the potentiometer reading is equivalent to $\pm 0.25^\circ\text{C}$. However upon considering the standard deviation of the constants in the linear equations, derived from the least squares analyses of the thermocouples calibrations, the derived standard deviation in the temperature is $\pm 1.6^\circ$.

The assumption of ideal behavior of SiF_4 under the conditions of the experiment is valid since the partial pressures are low even at

the highest temperature of this study. Also, the measurements were made under equilibrium conditions as discussed before.

Derived Thermodynamic Properties

The thermodynamic properties of $\text{BaSiF}_6(s)$ derived from measurements associated with the decomposition pressures and their temperature dependence are the enthalpy of formation, the free energy of formation, and the entropy all at the median temperature (655°K). The following thermodynamic data are needed to derive the above properties.

Thermodynamic data for $\text{BaF}_2(s)$

The enthalpy of formation of $\text{BaF}_2(s)$ at 298°K is -286.9 kcal mole⁻¹¹³. The enthalpy of formation at 655°K was calculated from equation¹⁴

$$\Delta H_f^\circ = -287,000 + 0.14T + 4.13 \times 10^{-3}T^2 - 0.80 \times 10^5 T^{-1} \quad (\text{III-6})$$

to be -285.3 kcal mole⁻¹.

The free energy of formation of $\text{BaF}_2(s)$ at 298°K is -274.5 kcal mole⁻¹¹⁴ and the calculated free energy of formation at 655°K according to equation¹⁴:

$$\Delta G_f^\circ = -287,000 - 0.14T \ln T - 4.13 \times 10^{-3}T^2 - 0.40 \times 10^5 T^{-2} \quad (\text{III-7})$$

is -260.2 kcal mole⁻¹.

The entropy of $\text{BaF}_2(s)$ at 298°K is 23.03 eu¹⁴ and the calculated entropy at 655°K from the equation:

$$S_T^\circ = S_{298}^\circ + \int_{298}^T dS = S_{298}^\circ + \int_{298}^T \frac{C_p}{T} dT \quad (\text{III-8})$$

is 37.74 eu. The molal heat capacity in the temperature range 298 to 1300°K is given by:

$$C_p = 13.98 + 10.20 \times 10^{-3}T \quad (\text{III-9})$$

Thermodynamic data for $\text{SiF}_4(\text{g})$

The enthalpy of formation of $\text{SiF}_4(\text{g})$ at 298° is -385.98 kcal mole⁻¹¹⁵ and the calculated value at 655°K by interpolation of the tabulated data from JANAF tables¹⁶, is -386.29 kcal mole⁻¹. The free energy of formation of $\text{SiF}_4(\text{g})$ at 298°K is -375.855 kcal mole⁻¹ and at 655°K is -363.325 kcal mole⁻¹¹⁶. The entropy of $\text{SiF}_4(\text{g})$ at 298°K is 67.433 eu and at 655°K is 83.482 eu¹⁶.

Thermodynamic properties of $\text{BaSiF}_6(\text{s})$

The equilibrium constant equation:

$$\log K_p = -(8238 \pm 183)T^{-1} + (9.978 \pm 0.120) \quad (\text{III-5})$$

is related to the thermodynamic properties of the decomposition of BaSiF_6 by:

$$\frac{\Delta G_T^\circ}{2.303 RT} = -\log K_p = \frac{\Delta H_T^\circ}{2.303 RT} - \frac{\Delta S_T^\circ}{2.303 R} \quad (\text{III-10})$$

The thermodynamic properties of the decomposition reaction at the median temperature, 655°K derived from the experimental data of equation (III-5) are:

$$\Delta H^\circ(655) = 37.67 \pm 0.84 \text{ kcal mole}^{-1},$$

$$\Delta S^\circ(655) = 45.65 \pm 0.55 \text{ eu},$$

$$\Delta G^\circ(655) = 7.77 \pm 0.9 \text{ kcal mole}^{-1}.$$

The cited errors in ΔH° and ΔS° are standard deviations from the

least squares analysis of the data, and in ΔG° is the propagated error using the above standard deviations.

From the above values and the corresponding values for $\text{BaF}_2(\text{s})$ and $\text{SiF}_4(\text{g})$ the following thermodynamic properties of BaSiF_6 at 655°K were derived:

$$\begin{aligned}\Delta H_f^\circ \quad (\text{BaSiF}_6, 655^\circ\text{K}): & -710.22 \pm 1.03 \text{ kcal mole}^{-1}, \\ \Delta G_f^\circ \quad (\text{BaSiF}_6, 655^\circ\text{K}): & -631.33 \pm 0.9 \text{ kcal mole}^{-1}, \\ S_{655}^\circ \quad (\text{BaSiF}_6) & : 75.57 \pm .55 \text{ eu.}\end{aligned}$$

The cited uncertainties are propagated errors based on the standard deviations of the decomposition thermodynamic functions and the errors in the thermodynamic properties listed in the literature for $\text{SiF}_4(\text{g})$.

Discussions and Conclusions

The partial pressures of $\text{SiF}_4(\text{g})$ in equilibrium with $\text{BaSiF}_6(\text{s})$ were calculated from the transpiration data in the temperature range 618 to 691°K . The values presented in Table IV are most likely to represent the minimum limit. Although the nonvolatile impurities, such as BaO and SiO_2 , present in the sample (Appendix D) don't contribute to the weight loss of the sample they are expected to decelerate the rate of evolution of $\text{SiF}_4(\text{g})$. Also the accumulation of $\text{BaF}_2(\text{s})$ on the sample surface might add to this effect. Although the amount of $\text{BaF}_2(\text{s})$ formed during the period of an experiment did not seem to lower the rate of decomposition significantly, its effect was checked quantitatively. The addition of 13.66 mole percent of $\text{BaF}_2(\text{s})$ to a sample of BaSiF_6 was found to lower the rate of weight loss by 16% which corresponds to a lowering of the partial pressure by 15.7%. The effect of the

accumulation of $\text{BaF}_2(\text{s})$ was studied under vacuum by Kana'an¹⁷ in an independent study of the decomposition of BaSiF_6 . The rate of decomposition in a Knudsen cell at isothermal conditions in the temperature range 620 to 690°K was measured. The observations indicated a constant rate of weight loss up to 37.5% of the total weight loss at 690°K and 15.3% at 620°K. After these percentages of weight loss, the rate dropped significantly and leveled off. Complete decomposition after extended periods was not possible. The maximum decomposition based on a 100% pure sample was approximately 80%. However on the basis of the actual purity of the sample (82% - Appendix D) the decomposition is considered to be complete. Using the same system Kana'an found that the effect of 20 mole % of BaF_2 added to the sample lowered the rate of weight loss by 5%. Thus the reported partial pressures of SiF_4 may be considered accurate within $\pm 5\%$.

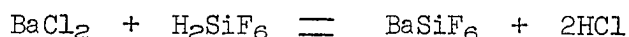
The derived enthalpy of the reaction might not be significantly different from the actual assuming that the slope of $\log K_p$ vs T^{-1} is not affected. However the derived entropy and free energy of the reaction might be lowered by 0.4 eu and 0.22 kcal mole⁻¹ respectively. In the absence of any reported thermodynamic values for BaSiF_6 the calculated thermodynamic properties of BaSiF_6 are acceptable within ± 1.1 kcal mole⁻¹ for ΔG_f° and ± 0.9 eu for S_{655}° .

The activation energy for decomposition of BaSiF_6 , reported by Deadmore et.al.³, at 560°C, is lower than the calculated enthalpy of decomposition by 5 kcal mole⁻¹. A difference between the energy of activation and the enthalpy change of an endothermic reaction should be in the opposite direction. Such inconsistency is unexplainable

without suspecting the validity of the reported activation energy.

Recommendations for Future Work

More accurate data might be obtained by using a sample of high purity. Apparently commercial samples are not expected to be of better quality. A pure sample might be obtained from preparations on a small scale by the reaction



Some improvements might be desirable in the furnace to widen the isothermal zone.

A detailed study of the effect of added BaF_2 to a sample of BaSiF_6 is recommended. The observed decrease in the rate of decomposition might be due to a change in the activity at the condensed phase surface or to a change in the equilibrium pressure. The dependence of the range of flow rates in the plateau region (in the curve of the rate of weight loss vs. flow rate) on the percentage of BaF_2 in the sample should be examined in the temperature range 600-700°K.

A check on the validity of the thermodynamic data for the reaction requires a knowledge of the thermodynamic properties of BaSiF_6 . These properties could be obtained from calorimetric measurements of the enthalpy of formation and the specific heat capacity at temperatures below 275°C where BaSiF_6 is thermally stable.

The partial pressures might be measured by decomposition studies in a static system using a quartz helix gauge or a diaphragm gauge.

Similar studies of other members of the hexafluorosilicates of groups I and II, especially those which are stable at the dehydration

temperatures of 110°-150°C, should reveal interesting trends regarding the thermal stability of these compounds.

APPENDICES

APPENDIX A

Flowmeter Calibration

The dibuthylphthalate capillary-flowmeter used was 9.7-cm long and 0.5-mm in diameter. The calibration was by the water displacement method. Argon was used as the flow calibration gas and distilled water as the displaced liquid. The arrangement used was the same flow system described in Figure 2. Argon flow discharged down-stream into the top of the water container. The displaced water was collected through a siphon tube, in a volumetric flask. Each measurement of a given flow rate was done as follows.

1. The flow line between the displaced water-container and the collector was cleared of trapped air-bubbles.
2. The flow rate was adjusted for a given constant difference in the oil levels in the flowmeter u-tube.
3. The volumetric flask was moved under the siphon-discharge and simultaneously an electric timer was started.
4. As the volumetric flask was filled to its volumetric mark the timer was stopped.

The volume was obtained directly from the volumetric flask capacity. The manometer reading, the barometric pressure, and the argon temperature were recorded.

The data were fitted into a linear least squares equation:

$$Q \text{ (cc min.}^{-1}\text{)} = a + bh \quad (\text{A-1})$$

where $a = 0.037 \pm 0.0015$

$$b = 2.473 \pm 0.037$$

and h is the difference in the oil level in the flowmeter u-tube in

cm. The standard deviation in Q is ± 0.23 cc min.⁻¹.

The data are presented in Table V.

TABLE V

Flowmeter Calibration at Experimental Conditions

h (cm)	Q (cc/min.)
1.60	3.79
2.85	6.69
3.10	7.85
3.45	8.85
3.85	9.70
5.15	12.92
6.53	16.00
7.80	19.45
8.85	22.00
11.85	29.18

APPENDIX B

Temperature Profile in the Reaction Region of the Furnace

The temperature distribution along the reaction cell was determined at several temperatures which are all above the temperature of the present study. The experimental thermocouple was at its fixed position. The reference thermocouple was inserted into the transpiration assembly, inside a tube which replaced the capillary of the composite tube and the condenser. At a given temperature, the emf output of the fixed experimental thermocouple was compared with that of the reference thermocouple. Each comparison was with the reference thermocouple junction at a different position along the reaction cell. The comparisons were over the length of the reaction cell, at 0.5" intervals. An isothermal zone within $\pm 3.5^\circ$ at 973°K and $\pm 3^\circ$ at 733°K was found over a 2.5" region in the reaction cell. At the lower temperatures of the present study ($618\text{-}691^\circ\text{K}$) the sample temperature is expected to be known to better than $\pm 3^\circ$.

APPENDIX C

Calibration of the Experimental- and Reference- Thermocouples

The reference thermocouple was calibrated against a standard thermocouple by placing the hot junctions of both thermocouples tip to tip at a position corresponding to the center of a tubular furnace. The calibration was under vacuum.

The cold junctions were at the ice-point well of an Ice-Point Reference System (Joseph Kaye and Co., Inc., Model RCS⁴). The emf measurements of both thermocouples were made with the same potentiometer (Honeywell Model 2745). The readings used for a linear least squares analysis were the average of 6-10 readings at the same temperature taken once every fifteen minutes.

The experimental thermocouple was calibrated against the reference thermocouple with the latter at the center of the reaction cell in the transpiration assembly. This calibration was part of the determination of the furnace profile.

The calibration data are presented in Tables VI and VII.

TABLE VI

Calibration of the Experimental Thermocouple in the
Transpiration Furnace Against the Reference Thermocouple

emf of the reference T.C. (mv)	emf of the experimental T.C. (mv)
14.28	14.37
15.08	15.19
15.88	16.02
16.69	16.87
17.37	17.57

TABLE VII

Calibration of the Reference Thermocouple
Against the Standard Thermocouple

emf of the standard T.C. mv	emf of the reference T.C. mv
13.85	14.04
14.67	14.85
15.43	15.60
16.21	16.37
17.03	17.17

APPENDIX D

Analysis of Barium Hexafluorosilicate

Dried samples of BaSiF_6 were qualitatively and quantitatively analyzed by x-ray and emission spectroscopy and by analysis for the elements respectively. X-ray diffraction patterns were shown to correspond to x-ray patterns of BaSiF_6 (Table VIII)¹⁸. X-ray diffraction patterns of a sample after complete decomposition (which accounted only for 78-80% of the theoretical weight loss) were shown to correspond to the x-ray patterns of BaF_2 (Table IX)¹⁹. However the x-ray method is not sensitive in detecting impurities of the order of 10% or less.

Qualitative atomic spectral analysis of both the original and the completely decomposed samples showed the presence of barium and silicon and an impurity of calcium.

Quantitative analysis for barium, silicon, fluorine and calcium were performed by Midwest Micro-lab, Inc. and showed that the sample is 90.6% Ba, Si and F and 0.6 Ca. The deficit was attributed to oxygen present in the form of oxides, mostly BaO and SiO_2 . The percentages of the elemental components were 43.6% Ba, 33.4% F and 13.7% Si. The corresponding theoretical values are 49.15% Ba, 40.80% F and 10.05% Si. If all the Ba in the sample was present as BaSiF_6 , then for 43.6% Ba, the corresponding fluorine and silicon should be 36.19% and 8.91%. Such assumption is invalid since the percentage of fluorine in the sample is less than 36.19%. On the other hand, the percentages of barium and silicon would be 40.2% and 8.2% respectively assuming that

all fluorine in the sample is in the form of BaSiF_6 . If the difference between these values and the experimental values is in the form of BaO and SiO_2 , the percentage of oxygen in the sample as such accounts for 6.8% of the total deficit. This leaves about 1.9% out of 8.7% not accounted for.

If calcium is in the form of CaF_2 , and the distribution of fluorine in the sample is reconsidered then the percentage of BaSiF_6 in the sample would be 80.4% instead of 81.6% according to the above arguments. Also the percentage of oxygen in the sample would be 6.9% instead of 6.8%. Either assumptions leaves about 2% of the sample not accounted for.

On the basis of the Midwest Microlab analysis, the sample is 81.8% BaSiF_6 . This explains the low percentage of weight loss (78-80%) after complete exhaustion of the sample with prolonged heating.

TABLE VIII

X-Ray Diffraction Data of BaSiF₆ Sample
Prior to Decomposition

D-Spacings Å	
Measured Values	Literature Values ¹⁸ for BaSiF ₆
4.64	4.650
3.58	3.593
3.04	3.055
2.85	2.845
2.23	2.230
2.07	2.075
1.95	1.953
1.79	1.796
1.54	1.548
1.52	1.527
1.49	1.519
1.42	1.422
1.40	1.405
1.36	1.358
1.32	1.322
1.23	1.230
1.20	1.197
1.17	1.174
1.16	1.163
1.11	1.111
Plus ten more lines between 1.06 and 0.79.	Some other lines reported with low intensities were not observed.

TABLE IX

X-Ray Diffraction Data of BaSiF_6 Sample
after Decomposition

D-Spacings \AA	
Measured Values	Literature Values ¹⁹ for BaF_2
3.54	3.579
3.05	3.100
2.16	2.193
1.85	1.870
1.77	1.790
1.53	1.550
1.41	1.423
1.37	1.386
1.25	1.266
1.18	1.193
1.08	1.095
1.05	1.048
1.02	1.033
0.976	0.980
0.936	0.945
0.926	0.935
too weak	0.895
0.861	0.868
too weak	0.860
0.824	0.824
0.803	0.807

BIBLIOGRAPHY

1. Truchot, Compt. Rend., 98, 821 (1884).
2. J. C. Bailar Jr. (ed.), Inorganic Synthesis Vol. IV, McGraw-Hill Book Co. Inc., N.Y., (1953), pp. 145-146.
3. D. L. Deadmore, J. S. Machin, and A. W. Allen, J. Amer. Ceramic Soc., 45, 120 (1962).
4. G. N. Lewis and M. Randall, Thermodynamics 2nd. ed. (revised by K. S. Pitzer and L. Brewer) McGraw-Hill Book Co., N.Y., (1961), p. 173.
5. H. V. Regnault, Ann. Chim., 15, 129 (1845).
6. G. W. Thomson, "Determination of Vapor Pressure" in Technique of Organic Chemistry, Vol. 1, A. Weissberger, (ed.), 3rd edition, Interscience, N.Y. (1959), pp. 401-522.
7. U. Merten and W. E. Bell in The Characterization of High Temperature Vapors, J. L. Margrave, (ed.), John Wiley and Sons, Inc., N.Y. (1967), pp. 91-114.
8. L. Brewer and N. L. Lofgren, J. Amer. Chem. Soc., 72, 3038 (1950).
9. K. A. Sense, C. A. Alexander, R. E. Bowman, and R. B. Filbert Jr., J. Phys. Chem., 61, 337 (1957).
10. D. Cubicciotti, J. Phys. Chem., 64, 791 (1960).
11. C. B. Alcock, and G. W. Hooper, Proc. Roy. Soc. (London), A254, 551 (1960).
12. W. E. Bell, M. C. Garrison and U. Merten, J. Phys. Chem., 65, 517 (1961).

13. L. Brewer, G. R. Somayajulu and E. Brackett, Chem. Rev., 63, 111 (1963).
14. C. E. Wicks and F. E. Block, Bulletin 605 Bureau of Mines (1963); p. 17.
15. S. S. Wise, J. L. Margrave, H. M. Feder and W. N. Hubbard, J. Phys. Chem., 67, 815 (1963).
16. D. R. Stull, JANAF Thermochemical Tables (1965).
17. A. S. Kana'an (unpublished work, 1969).
18. J. V. Smith (ed.), Index (Inorganic) to the Powder Diffraction File, American Society for Testing and Materials, Philadelphia, Pa., (1966), data card 15-736, p. 466.
19. J. F. Smith (ed.), X-Ray Powder Data File, Sets 1-5 (Revised) Inorganic, Vol. PD1S 5iRB, American Society for Testing and Materials, Philadelphia, Pa., (1967), data card 4-0452, p. 513.